Available online at www.sciencedirect.com

ScienceDirect

Journal of Genetics and Genomics 41 (2014) 357−368

JGG

ORIGINAL RESEARCH

The E3 Ubiquitin Ligase gp78 Protects against ER Stress in Zebrafish Liver

Zhiliang Chen [a,b], Petek Ballar [c], Yu Fu [d], Jia Luo [e], Shaojun Du [f,*], Shengyun Fang [a,b,*]

[a] *Center for Biomedical Engineering and Technology, Baltimore, MD 21202, USA*
[b] *Department of Physiology, University of Maryland School of Medicine, Baltimore, MD 21201, USA*
[c] *Faculty of Pharmacy, Biochemistry Department, Ege University, Izmir 35100, Turkey*
[d] *Biopharmaceutical Research Institute, Anhui Medical University, Hefei 230032, China*
[e] *Department of Internal Medicine, University of Kentucky College of Medicine, Lexington, KY 40536, USA*
[f] *Department of Biochemistry and Molecular Biology, University of Maryland School of Medicine, Baltimore, MD 21202, USA*

Received 22 April 2014; revised 3 May 2014; accepted 4 May 2014
Available online 2 June 2014

ABSTRACT

Enhanced endoplasmic reticulum (ER)-associated protein degradation (ERAD) activity by the unfolded protein response (UPR) represents one of the mechanisms for restoring ER homeostasis. *In vitro* evidence indicates that the mammalian gp78 protein is an E3 ubiquitin ligase that facilitates ERAD by polyubiquitinating and targeting proteins for proteasomal degradation under both physiologic and stress conditions. However, the *in vivo* function of gp78 in maintaining ER protein homeostasis remains untested. Here we show that like its mammalian counterpart, the zebrafish gp78 is also an E3 ubiquitin ligase as revealed by *in vitro* ubiquitination assays. Expression analysis uncovered that *gp78* is highly expressed in several organs, including liver and brain, of both larval and adult fish. Treatment of larvae or adult fish with tunicamycin induces ER stress and upregulates the expression of several key components of the gp78 ERAD complex in the liver. Moreover, liver-specific overexpression of the dominant-negative form of gp78 (gp78-R2M) renders liver more sensitive to tunicamycin-induced ER stress and enhances the expression of sterol response element binding protein (Srebp)-target genes, which was largely suppressed in fish overexpressing wild-type gp78. Together, these data indicate that gp78 plays a critical role in protecting against ER stress in liver.

KEYWORDS: Zebrafish; gp78/AMFR; UPR; Lipogenesis; Cholesterol; ERAD

The quality of proteins destined for the secretory pathway is tightly monitored by the endoplasmic reticulum (ER) quality control (ERQC) system (Vembar and Brodsky, 2008). Misfolded proteins are recognized in the ER, retrotranslocated, polyubiquitinated, and then targeted for degradation by the 26S proteasome in the cytosol. This is a complicated process termed ER-associated protein degradation (ERAD) (Vembar and Brodsky, 2008). Inefficient clearance of misfolded proteins leads to their accumulation in the ER lumen, which induces ER stress. The latter activates the unfolded protein response (UPR), a signaling transduction pathway that restores ER protein homeostasis (Malhotra and Kaufman, 2007; Walter and Ron, 2011). The UPR has been shown to exist in organisms from yeast to human.

gp78 is a polytopic RING (really interesting new gene) finger protein in the ER (Shimizu et al., 1999; Ponting, 2000; Fang et al., 2001). It protects cultured cells against ER stress by facilitating ERAD. On the other hand, acute ER stress enhances gp78-mediated ERAD by suppressing its autoubiquitination,

* Corresponding authors. Tel: +1 410 706 2220, fax: +1 410 706 8184 (S. Fang); Tel: +1 410 234 8854, fax: +1 410 234 8896 (S. Du).
E-mail addresses: sdu@som.umaryland.edu (S. Du); sfang@umaryland.edu (S. Fang).

http://dx.doi.org/10.1016/j.jgg.2014.05.005

leading to its stabilization (Shen et al., 2007). gp78 also counteracts ER stress induced by non-ER neurodegenerative disease proteins, including mutant superoxide dismutase 1 (SOD1), ataxin-3 and huntingtin. gp78 represses the aggregation and enhances the degradation of these mutant proteins (Ying et al., 2009; Yang et al., 2010). In addition to being an ERAD E3, gp78 has been reported to be the receptor for the tumor autocrine motility factor (AMF) to promote metastasis. Treatment with AMF protects cells against tunicamycin-induced ER stress and this protection is mediated by gp78 (Fu et al., 2011).

gp78 plays important roles in liver function. It acts as an E3 for ERQC of proteins in liver. gp78 increases the solubility and enhances the degradation of the Z variant of α-1-antitrypsin, lack of which is the primary cause of α-1-antitrypsin deficiency (Shen et al., 2006). gp78 has also been reported to be involved in proteasomal degradation of cytochrome P450 3A (CYP3A), a cytochrome P450 enzyme responsible for drug metabolism in the liver. In addition, gp78 has been implicated in proteasomal degradation of liver cytochrome P450 2E1 (CYP2E1), which is responsible for the biotransformation of clinically relevant drugs, low molecular weight xenobiotics, carcinogens and endogenous ketones, in cultured rat hepatocytes (Kim et al., 2010; Peer et al., 2011; Wang et al., 2011). Moreover, gp78 is involved in regulating degradation of important liver proteins. For example, very low density lipoproteins (VLDL) is a major secretory product of the liver, which acts as a transporter of endogenously synthesized lipids, mainly triglyceride. Apolipoprotein B-100 (apoB-100) availability is a key determinant of VLDL secretion. gp78 targets apoB-100 to the ERAD pathway for degradation when lipid availability limits assembly of VLDLs (Fisher et al., 2011). gp78 facilitates sterols- and insig1-dependent degradation of HMG-CoA reductase (Song et al., 2005), a rate-limiting enzyme in the synthesis of cholesterol and nonsterol isoprenoids. gp78 also targets insig1 to the ERAD pathway when sterols are depleted. Similar regulations have been reported in *gp78*-knockout mice (Liu et al., 2012). However, the regulation of HMG-CoA reductase by gp78 was not confirmed in *gp78*-knockout mouse embryonic fibroblasts (Tsai et al., 2012). In *gp78* transgenic mice, a hyperplastic phenotype was observed in mammary glands and no phenotype in liver was described (Joshi et al., 2010). So far, the significance of gp78 in the regulation of ER stress under physiologic or stress conditions *in vivo* has not been reported.

The zebrafish has been shown to be an ideal system for studying hepatic ER stress, lipid metabolism, hepatic steatosis, and alcoholic or non-alcoholic fatty liver disease for the following reasons: facility of exposing to chemicals, the sensitivity of its liver to environmental perturbation, the lack of effect of external nutrients on its liver functions during early developmental stages, easy genetic manipulation, such as the generation of transgenic models, knockdown of gene expression by morpholinos, and being relatively easy to generate gene-specific mutation by transcription activator-like effector nuclease (TALEN) (Lieschke and Currie, 2007; Passeri et al., 2009; Cinaroglu et al., 2011; Thakur et al., 2011; Huang et al., 2012; Howarth et al., 2012; Wei et al., 2013).

In this study, we analyzed the regulatory role of gp78 in embryonic development and hepatic ER stress in zebrafish. We demonstrated that inhibition of gp78 expression or function neither affects embryonic development nor causes hepatic ER stress under normal physiologic conditions. However, blocking gp78 function by a dominant-negative gp78 renders liver more sensitive to tunicamycin-induced ER stress. Moreover, the sensitization to ER stress is accompanied by the upregulation of Srebp (sterol response element binding protein) target genes, suggesting a potential role for gp78 in the regulation of hepatic lipid homeostasis through activation of Srebp pathway under stress conditions. Using transgenic fish that overexpress the dominant-negative form of gp78 in the liver, we found that the gp78-mediated ERAD pathway plays a key role in the regulation of hepatic ER stress and lipid metabolism.

The *gp78* cDNA was isolated from zebrafish larvae at 5 dpf (days post fertilization) by RT-PCR. The zebrafish *gp78* gene encodes a protein of 620 amino acids that shares high sequence identity with gp78 from frog, mouse, and human (Ballar et al., 2010). Zebrafish gp78 is predicted to have five transmembrane domains at the N-terminal region and five other functional domains in the cytosolic-tail (Fig. 1A). The five additional domains include a RING finger, an oligomerization site (OS), a coupling of ubiquitin to ER degradation (Cue) domain, a ubiquitin-conjugating enzyme E2 G2 (Ube2g2)-binding region (G2BR) and a p97/VCP-interacting motif (VIM) (Fang et al., 2001; Ballar et al., 2006; Das et al., 2009; Li et al., 2009). Sequence comparison shows that all these domains are highly conserved among zebrafish, frog, mouse, and human (Chen et al., 2012). Amino acid sequence comparison reveals that zebrafish and human gp78 have 94%, 97%, 81%, 50%, and 48% identity for the RING, OS, Cue, G2BR, and VIM domains, respectively (Fig. 1B), suggesting that gp78 function might be conserved during evolution.

Since zebrafish contains all the conserved domains of mammalian gp78, we next determined whether zebrafish gp78 is an ER-localized E3 ubiquitin ligase. The subcellular localization of gp78 was determined by immunostaining. The results showed that zebrafish gp78, like human gp78, colocalized with mouse MmUBC7, which is the cognate E2 localized to the ER in HeLa cells (Fig. 2A−B). The E3 ubiquitin ligase activity of gp78 was determined by *in vitro* polyubiquitination assay using recombinant gp78-GST proteins. As shown in Fig. 2C, the recombinant cytosolic tail of zebrafish gp78-C fused with GST as its human ortholog, exhibited the activity to promote the formation of polyubiquitin chains *in vitro*, confirming that zebrafish gp78 indeed acts as an E3 ubiquitin ligase.

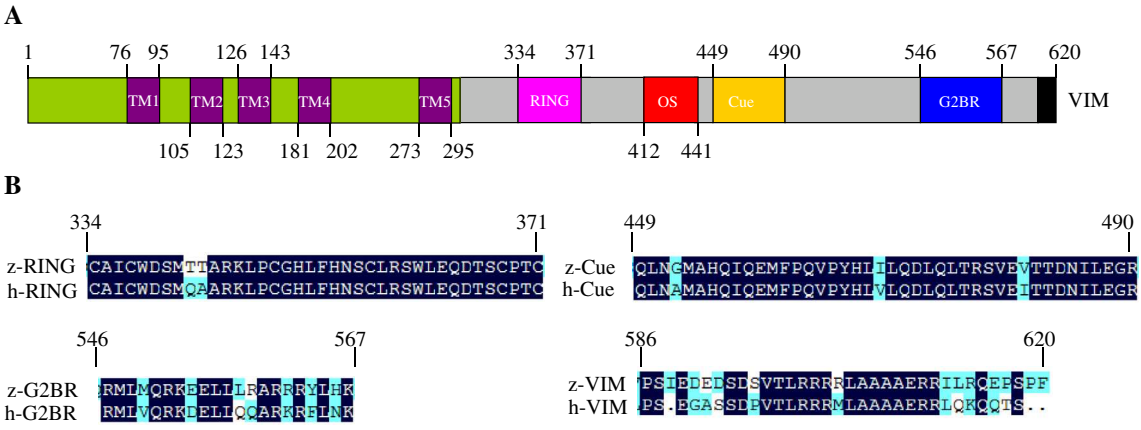

A: The zebrafish gp78 contains 5 transmembrane domains (TMs) and 5 conserved domains in the cytosolic tail. The TMs were predicted using TMHMM-2.0. **B:** The protein sequence alignment of conserved domains in zebrafish and human gp78 proteins. These include the really interesting new gene (RING) finger domain (333−371), coupling of ubiquitin to ER degradation (CUE) domain (449−490), Ube2g2-binding region (G2BR; 546−567) and a p97/VCP-interacting motif (VIM; 586−620). Multiple sequence alignment was performed using DNAMAN.

The temporal expression of *gp78* was determined in zebrafish embryos by RT-PCR (Fig. 3A). *gp78* transcripts were detected in fertilized eggs. The expression of *gp78* remained constitutive at all embryonic and larval stages analyzed, from fertilization up to 6 dpf (Fig. 3A).

To determine the spatial expression patterns, we analyzed *gp78* expression in zebrafish embryos by whole-mount *in situ* hybridization (Fig. 3B−E). A 1125 nucleotides (nt) antisense

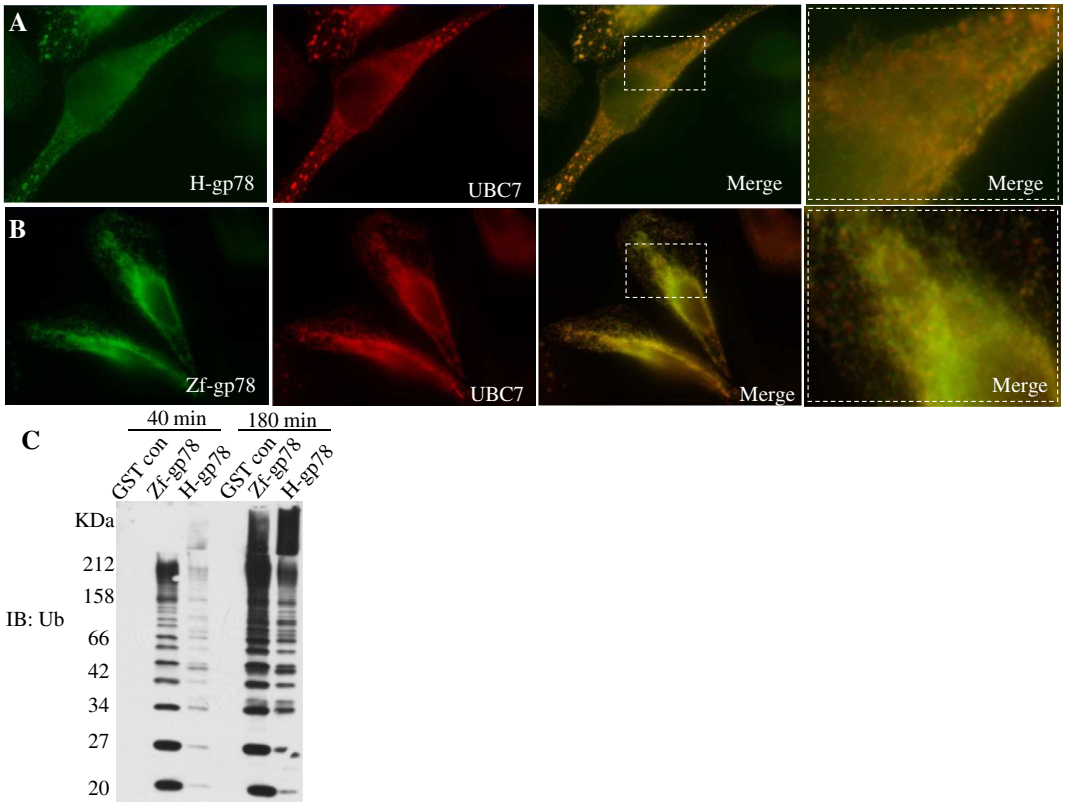

A and **B:** Flag-tagged zebrafish gp78 (flag-zf-gp78) and flag-tagged human gp78 (flag-h-gp78) colocalize with myc-tagged mouse MmUBC7 by double immunostaining using anti-flag and anti-myc antibodies in HeLa cells. The boxed areas in the third panel are enlarged and shown in the last panel. **C:** *In vitro* ubiquitination assay shows that recombinant His-tagged human gp78 (H-gp78) and GST-tagged zebrafish gp78 (Zf-gp78) promote the formation of polyubiquitin chains. GST protein was used as negative control (GST con).

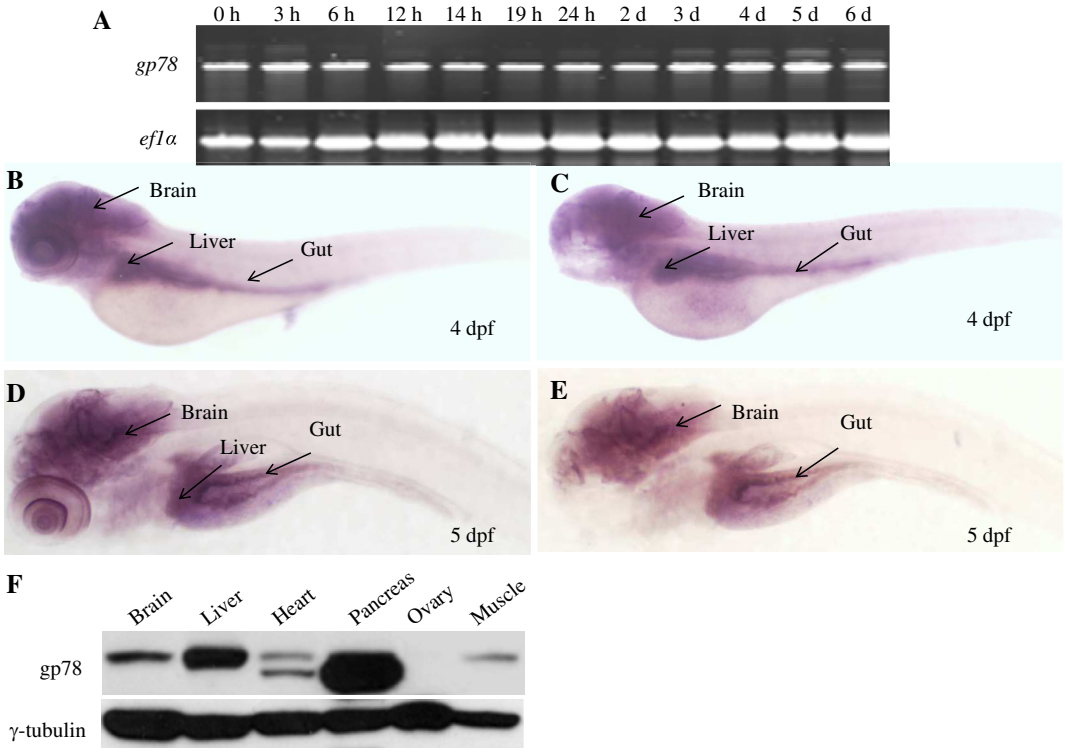

A: The *gp78* transcripts were detected in zebrafish embryos by RT-PCR during the first 6 days (d) of development. **B**−**E:** The spatial expression pattern of *gp78* in 4 dpf (**B** with eyes, **C** with eyes removed) and 5 dpf (**D** with eyes, **E** with eyes removed) embryos revealed by *in situ* hybridization using a dig-labeled *gp78* antisense probe. **F:** The tissue expression of gp78 protein was analyzed in adult zebrafish tissues by Western blot using the anti-gp78 monoclonal antibody 1F1. Interestingly, two bands were detected in the heart.

probe complementary to the 3′ end of the *gp78* RNA transcript was generated for *in situ* hybridization. *In situ* hybridization using the probe revealed *gp78* mRNA expression in several tissues including the brain, eyes, liver, gut, and pancreas of zebrafish embryos at 4 dpf and 5 dpf (Fig. 3B−E). Western blot analysis showed expression of gp78 in several tissues of adult zebrafish. A relatively high level of expression was found in the liver and pancreas (Fig. 3F), similar to the expression pattern in tissues of adult mice (not shown). Interestingly, two protein bands were detected by Western blot in the heart of zebrafish (Fig. 3F). This could come from the expression of alternatively spliced *gp78* mRNAs. Consistent with this idea, two types of *gp78* transcripts have been identified (data not shown).

Molecular chaperones and components of ERAD pathway are two major types of UPR target genes. To determine the effects of ER stress on genes of the gp78 complex, we exposed fish embryos to 1 μg/mL of tunicamycin, a protein N-glycosylation inhibitor and a well-known ER stress inducer for 48 h between 3−5 dpf as previously described (Passeri et al., 2009). Expression of ER stress markers including binding immunoglobulin protein (BiP) and CCAAT/enhancer-binding-protein-homologous protein (CHOP) was analyzed by whole-mount *in situ* hybridization. As shown in Fig. 4, an elevated expression of *bip* and *chop* was observed in the liver of fish larvae treated with tunicamycin (Fig. 4A−B). As expected, no change in expression was observed using a liver specific probe *fabp10a*, a non-UPR responsive gene (Fig. 4F). Similar to *bip* and *chop*, treating fish embryos with tunicamycin significantly upregulated the expression of genes encoding the known components of the gp78 complex, *gp78*, *derlin1* and *p97/VCP* (Fig. 4C−E). Interestingly, the increased expression was restricted to the liver of fish larvae in response to tunicamycin treatment.

Next, we examined whether tunicamycin treatment could induce ER stress markers and the expression of gp78 and its partners in the liver of adult zebrafish. Adult zebrafish (3 months) were exposed to 2.5 μg/mL of tunicamycin for 6, 12, 18, 14, 32 and 56 h. Expression of ER stress markers, *bip*, *chop* and spliced *X-box binding protein 1* (*xbp1*), was analyzed by RT-PCR. The results showed that exposing adult fish to tunicamycin for 12 h could significantly elevate the levels of *bip* and *chop* expression (Fig. 4G). However, the generation of alternatively spliced *xbp1*, another indicator of ER stress, could not be observed until 56 h of tunicamycin treatment (Fig. 4G and H). Similar to the data from larval exposure, increased levels of expression were also detected for *gp78*, *p97/VCP* and *derlin1* in the liver of adult fish treated with tunicamycin (Fig. 4G). Consistent with the results of mRNA expression, an increase of BiP and gp78 protein expression was observed by

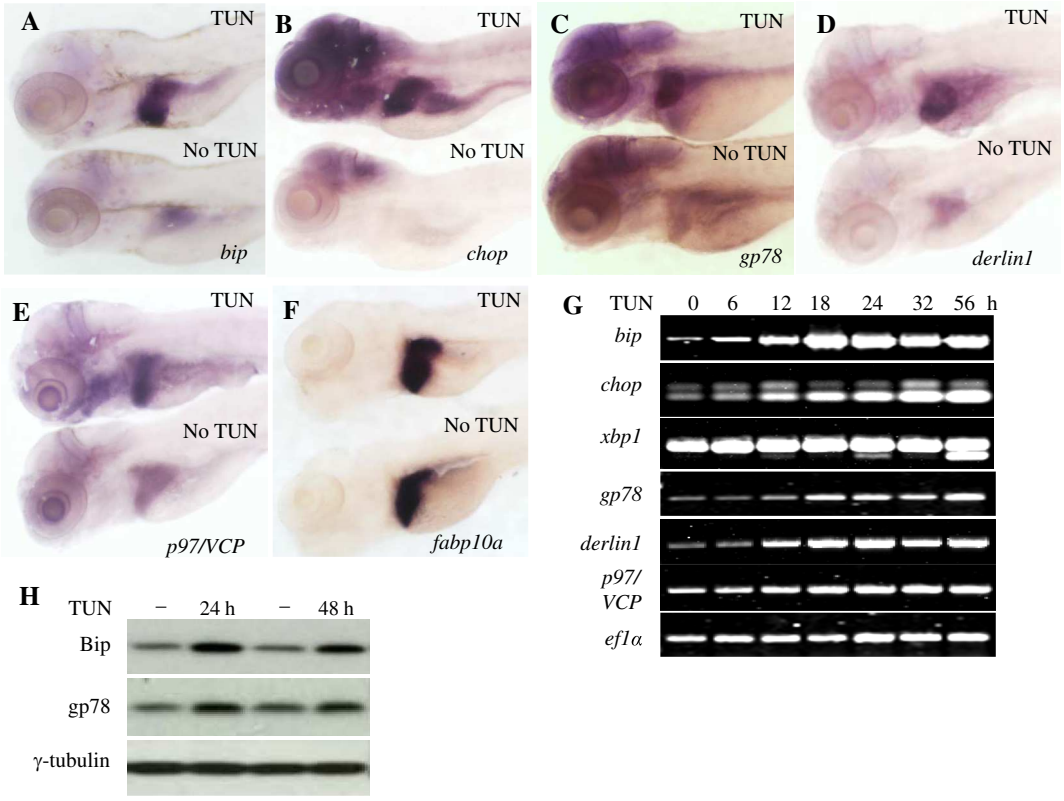

A−E: *In situ* hybridization shows the upregulation of the ER stress markers (*bip* and *chop*) and genes encoding the components of the gp78 complex, namely *gp78*, *derlin1*, and *p97/VCP*, in the liver of 5.5 dpf larvae treated with 1 μg/mL tunicamycin (TUN) for 48 h. **F:** *In situ* hybridization shows the normal expression of the fatty acid binding protein 10a (*fabp10a*) transcript, a non-UPR responsive gene specifically expressed in the liver as a control. **G:** RT-PCR result shows the upregulation of the ER stress markers *bip*, *chop*, and the spliced form of *xbp1* (*s-xbp1*), as well as genes encoding the components of the gp78 complex, *gp78*, *derlin1*, and *p97/VCP* in the livers of adult fish treated with 2.5 μg/mL TUN for the indicated periods of time. The expression level of elongation factor 1 alpha (*ef1α*) transcripts was used as an internal control. **H:** Western blot analysis shows an increase of Bip and gp78 protein levels in the liver of adult fish treated with 2.5 μg/mL TUN for 24 h and 48 h.

the Western blot analysis (Fig. 4H). Together, these data suggest that activation of the UPR by tunicamycin results in the upregulation of gp78 expression and its partners, which might coordinately enhance the degradation of misfolded proteins by gp78-mediated ERAD.

To study the *in vivo* function of gp78, we performed a knockdown analysis of *gp78* in zebrafish embryos. A morpholino translational blocker targeted to the 5′-UTR region was injected into zebrafish embryos at 1- to 2-cell stage. The effect on *gp78* knockdown was analyzed at different stages by Western blot (Fig. 5A and B). As shown in Fig. 5A, injection of the 5′-UTR morpholino dramatically inhibited gp78 protein expression at 24 and 48 hpf (Fig. 5A). The efficient inhibition was observed even at 96 and 120 hpf (Fig. 5B). To determine whether or not the knockdown of *gp78* causes gross developmental defects, the morphant embryos were examined morphologically every day for 7 days after the morphant injection. Compared with the control embryos, the morphant embryos appeared morphologically normal at 48 and 72 hpf (Fig. 5C and D) as well as at the early developmental stages and up to 7 dpf (data not shown).

Because of the high levels of gp78 expression in liver, we further investigated whether the knockdown of *gp78* affects liver development. The *Tg(hfe2:gfp)* transgenic line that expresses green fluorescent protein (GFP) specifically in the zebrafish liver was used to assay the effect of *gp78* knockdown (Bian et al., 2011). The morphant embryos showed normal liver formation at 96 hpf (Fig. 5E). To test whether the *gp78* knockdown morphant embryos were more sensitive to tunicamycin-induced stress, the gp78 morphant and control embryos were treated with tunicamycin between 48−96 hpf. No significant difference was detected in the control and morphant embryos in terms of overall morphology and liver development (Fig. 5F). These data suggest that gp78 might not be essential for the normal development and liver formation of zebrafish embryos.

To analyze gp78 function in hepatic ER stress in adult fish, we used a dominant-negative approach by expressing a gp78

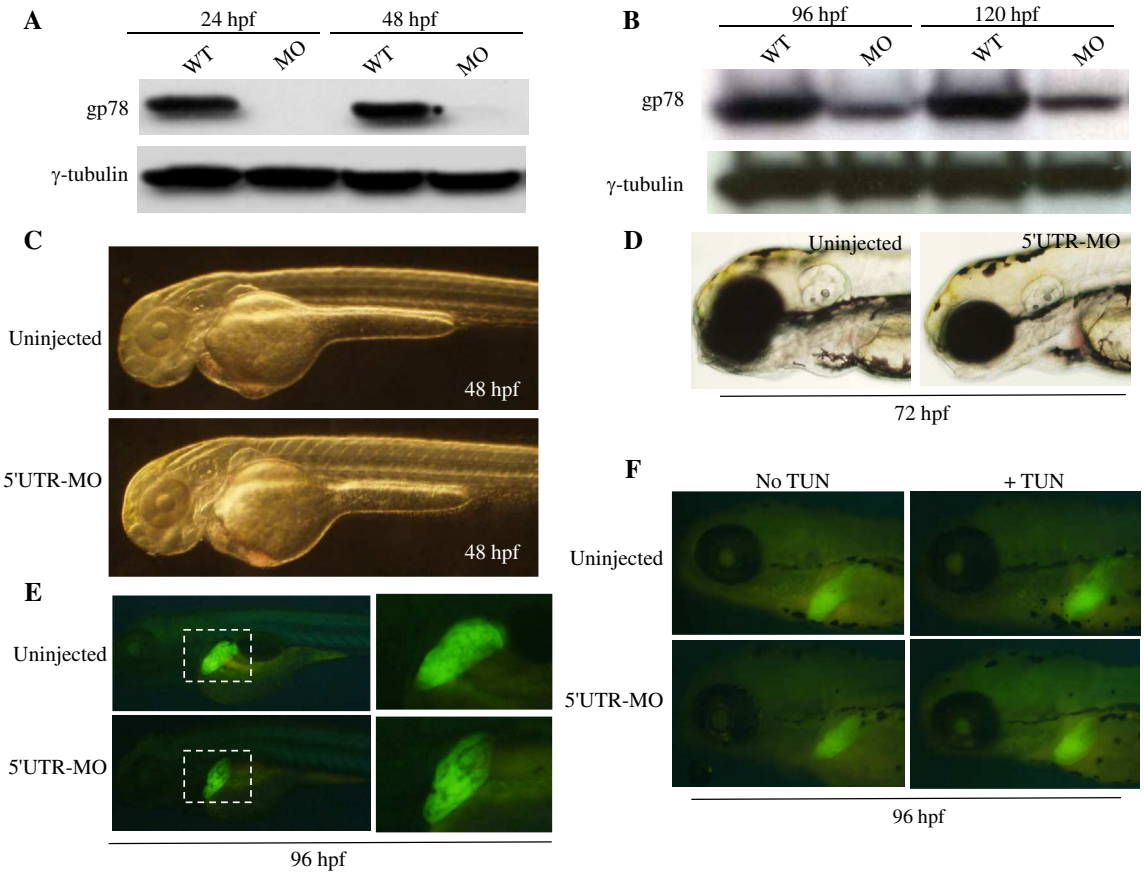

A and **B:** Western blot shows the levels of gp78 protein expression in *gp78* morpholino (MO) injected and control embryos at 24, 48, 96 and 120 hpf. **C** and **D:** Compared with the un-injected controls, the *gp78* morpholino injected embryos (5′UTR-MO) appeared morphologically normal at 48 and 72 hpf. **E:** Liver development revealed by GFP expression in uninjected and *gp78*-MO injected *Tg(hfe2:gfp)* transgenic embryos at 96 hpf. Higher magnification pictures of the boxed areas are shown on the right panel. **F:** Liver development in control and *gp78* knockdown *Tg(hfe2:gfp)* transgenic embryos growing in normal and tunicamycin (TUN)-induced stress conditions at 96 hpf.

dominant-negative mutant (gp78-R2M) specifically in the liver. The gp78-R2M mutant was generated by substitution of the H354 and H357 residues in the RING finger domain with asparagine residues. It has been shown that mutation of two zinc binding residues in the gp78 RING finger domain leads to dominant-negative effects on the degradation of several substrates, including CD3δ, CFTRΔF508, and HMG-CoA reductase (Fang et al., 2001; Song et al., 2005; Morito et al., 2008; Ballar et al., 2010). Transgenic zebrafish lines expressing the dominant-negative gp78 (gp78-R2M) and the wild-type gp78 (gp78-wt) were generated (Figs. S1 and S2). The expression of these transgenes in the liver of transgenic fish was confirmed by RT-PCR and Western blot analyses (Figs. S1B, C and S2B, C).

To determine whether overexpression of the gp78-R2M dominant-negative renders the liver more sensitive to ER stress, we first analyzed the expression of ER stress markers under normal physiologic conditions. Livers dissected from transgenic fish expressing the wild-type or mutant gp78 and their non-transgenic siblings were subjected to RT-PCR analysis for *bip* expression. As shown in Fig. 6, no significant difference in *bip* expression was observed in control and transgenic fish under normal physiologic conditions (Fig. 6A and D). However, under tunicamycin-induced ER stress conditions, the transgenic fish expressing the dominant-negative gp78 showed a significant increase in *bip* expression compared with non-transgenic control receiving the same tunicamycin treatment. As shown by semi-quantitative RT-PCR, exposing 2-month-old *Tg(gp78-R2M)* transgenic zebrafish to 2.5 μg/mL tunicamycin for 6 h significantly upregulated the expression of *bip* in the liver (Fig. 6A and D). In contrast, this increased *bip* expression was not observed in the non-transgenic control or transgenic fish expressing the wild-type gp78 (Fig. 6B and D). Collectively, these studies indicate that overexpression of gp78-R2M rendered adult zebrafish more sensitive to tunicamycin-induced hepatic ER stress.

It has been demonstrated that ER stress activates the SREBP transcription factors that are key regulators of fatty acid and cholesterol synthesis, in insulin- and alcohol-induced hepatic steatosis (Kammoun et al., 2009). Since we observed an enhanced hepatic ER stress in the *Tg(gp78-R2M)* transgenic

A and **B:** The effect of overexpressing gp78 dominant-negative (gp78-R2M) or wild-type gp78 (gp78-wt) in the fish liver on the expression of the ER stress marker *bip* in response to tunicamycin (TUN) treatment. Two-month-old adult transgenic fish expressing gp78-R2M or gp78-wt and their non-transgenic siblings were treated with or without 2.5 μg/mL TUN for 6 h. Livers were dissected and subjected to semi-quantitative RT-PCR for the ER stress marker *bip*. **C** and **D:** Quantitative data of (**A**) and (**B**) were analyzed. Symbol "−" represents non-transgenic fish. Symbol "+" represents transgenic fish. Gray bar represents data of **B**; black bar represents data of **A**. The neg and pos represent non-transgenic negative control and transgenic fish, respectively. The values were normalized to those in untreated non-transgenic fish.

fish in response to tunicamycin, we next analyzed the mRNA levels of Srebp target genes involved in the synthesis of fatty acids and cholesterol. RT-PCR analysis revealed that the mRNA levels of Srebp-1c and Srebp-2 target genes were dramatically increased in the liver of gp78-R2M-transgenic fish compared with wild-type fish after challenge with tunicamycin for 6 h (Fig. 7A and I). These include *acetyl coenzyme A carboxylase a* (*acc1*), *fatty acid desaturase* (*fads*), and *fatty acid synthase* (*fasn*) targeted by Srebp-1c as well as *3-hydroxy-3-methylglutaryl coenzyme A reductase a* (*hmgcra*), *3-hydroxy-3-methylglutaryl coenzyme A synthase 1* (*hmgcs1*) regulated by Srebp-2. After similar challenge with tunicamycin for 6 h, we also observed the upregulation of *srebp1* mRNA transcripts in the livers of gp78-R2M-transgenic fish (Fig. 7A and I). In contrast, overexpression of wild-type gp78 had little or no effect on the expression of *srebp1* and their target genes in response to tunicamycin-induced ER stress (Fig. 7B and C−J).

To test whether the increased expression of *srebp* and their target genes was due to tunicamycin-induced ER stress in the liver, we analyzed the expression of *cyp2e1*, a key enzyme in drug metabolism in liver but not an ER stress responsive gene. The results showed that there was no difference in *cyp2e1* expression in the livers from gp78-R2M-transgenic fish and the non-transgenic control receiving the same treatment with tunicamycin (Fig. 7A and K), indicating that the upregulation of Srebp target genes in the liver of gp78-R2M-transgenic fish is caused by ER stress in the liver.

In this study, we analyzed the regulatory role of gp78 in embryonic development and hepatic ER stress in zebrafish. It was found that inhibition of gp78 expression or function neither affects embryonic development nor causes hepatic ER stress under physiologic conditions. However, blocking gp78 function by a dominant negative in liver renders fish liver more sensitive to tunicamycin-induced ER stress. Moreover, the sensitization to ER stress is accompanied by the upregulation of Srebp target genes involved in lipogenesis and cholesterol synthesis, suggesting a potential role for gp78 in the regulation of hepatic lipid homeostasis through activation of Srebp pathway under stress conditions.

gp78 has been shown to target many different substrates, including misfolded and normal proteins, for degradation in cultured cells (Chen et al., 2012). It is surprising that knockdown

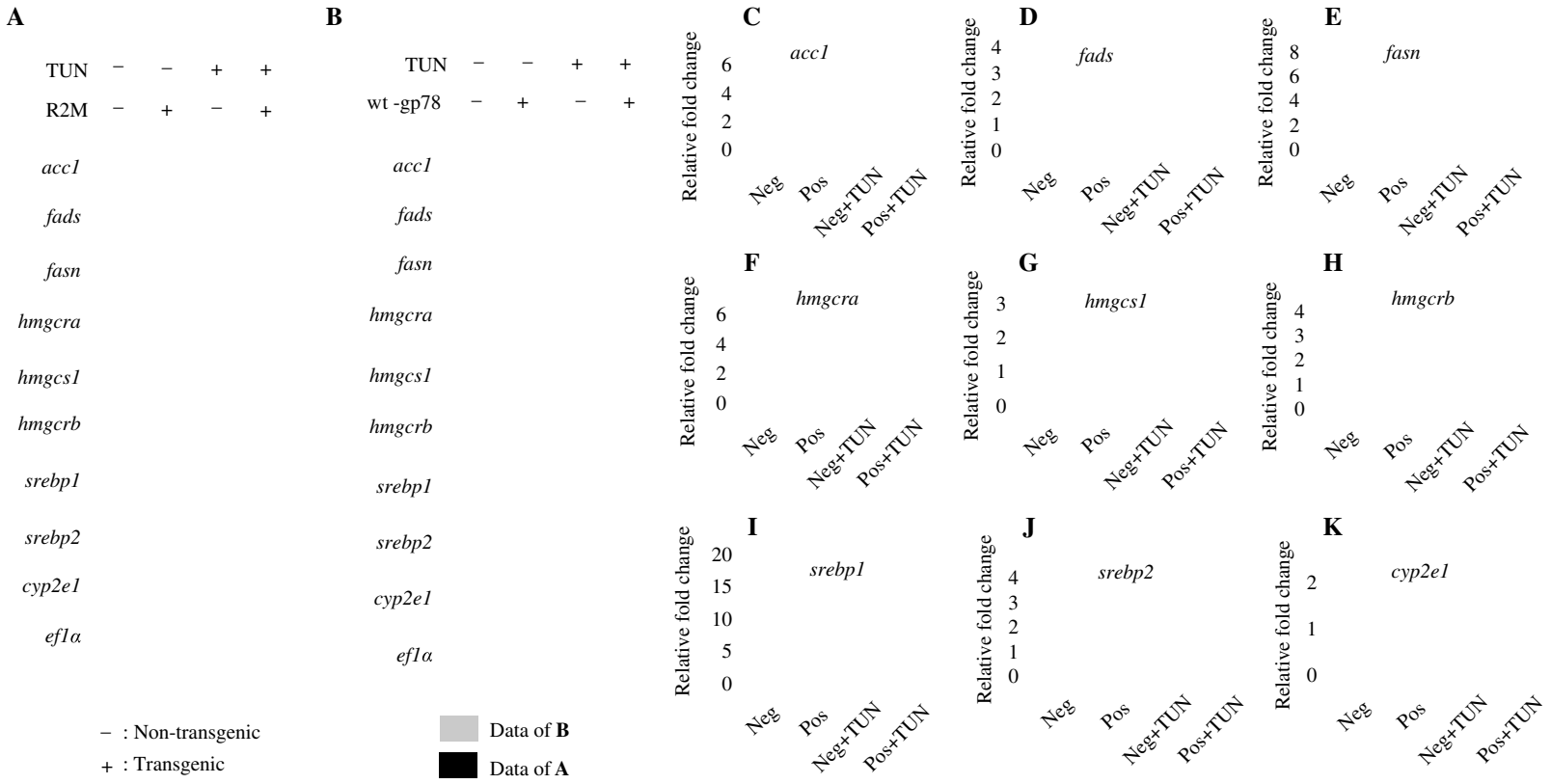

A and **B:** The effect of overexpressing gp78 dominant-negative (gp78-R2M) or wild-type gp78 (gp78-wt) in the fish liver on the expression of Srebp-1c target genes (*acc1*, *fads*, and *fasn*), and the Srebp-2 target genes (*hmgcra*, *hmgcs1* and *hmgcrb*, *srebp1*, *srebp2*, and *cyp2e1*). Two-month-old adult transgenic fish expressing gp78-R2M or gp78-wt and their non-transgenic siblings were treated with or without 2.5 μg/mL tunicamycin (TUN) for 6 h. Livers were dissected and subjected to semi-quantitative RT-PCR analysis. **C**–**K:** Quantitative data of (**A**) and (**B**) were analyzed. Symbol "**−**" represents non-transgenic fish. Symbol "**+**" represents transgenic fish. Gray bar represents data of **B**; black bar represents data of **A**. The neg and pos represent non-transgenic negative control, and transgenic fish, respectively. The values were normalized to those in untreated non-transgenic fish.

of *gp78* expression in zebrafish embryos does not result in morphological phenotypes under normal physiologic conditions. This is in contrast to a previous report that knockout of HMG-CoA reductase degradation protein-1 (Hrd1, also named as SYVN1, the human ortholog of Hrd1), a gp78 homolog E3 ubiquitin ligase, in mice results in embryonic lethality due to severe anemia (Yagishita et al., 2005), which is probably caused by enhanced apoptosis of embryonic erythrocytes in the liver (Amano et al., 2003; Yagishita et al., 2005). Importantly, our study in zebrafish is in agreement with the report in *Caenorhabditis elegans* that deletion of gp78 ortholog, *Hrdl-1*, has no phenotype (Sasagawa et al., 2007). The different phenotypes from loss of gp78 or Hrd1 function may reflect their differences in substrate spectrums. Compared with gp78, Hrd1 may cover a wider spectrum of substrates. Loss of gp78 function may be compensated by the presence of Hrd1. However, gp78 cannot replace Hrd1 because knockout of Hrd1 alone results in early embryonic lethality (Yagishita et al., 2005). Thus, understanding the substrate spectrums for gp78 and Hrd1 in animals may help to explain their different functional roles. Another surprising finding is that tunicamycin primarily induces ER stress in liver. We speculate that this preference is likely due to the easy accessibility of tunicamycin to liver compared with other organs in live fish. Zebrafish, thus, provides a good model for studying ER stress in liver.

Moreover, liver-specific overexpression of wild-type gp78 or the dominant negative does not induce hepatic ER stress under normal physiologic conditions. This result is consistent with a previous study showing that overexpression of the wild-type or mutant Hrd1 or gp78 alone does not induce ER stress in cultured cells (Bernardi et al., 2010). Similarly, the knockdown of *gp78* in HepG2 cells does not affect the levels of *bip, Hsp70* and *p97* expression (Fisher et al., 2011). Together, these data suggest that gp78 may not be required for the basal ERAD activity. Alternatively, other E3s, such as Hrd1 and TEB4, may compensate for the loss of gp78 function in basal ERAD activity (Kostova et al., 2007; Mehnert et al., 2010). The question is why overexpression of the dominant-negative gp78, gp78-R2M, sensitized liver to tunicamycin-induced ER stress. This could be due to the fact that different ERAD E3 complexes share important common components. For example, gp78 and Hrd1 share the key retrotranslocation factor p97/VCP. Overexpression of the dominant-negative gp78 could sequester p97/VCP *via* its p97/VCP-interacting motif (Ballar et al., 2006), thereby inhibiting the function of Hrd1 and possibly other E3s. Thus, in the presence of gp78 dominant negative, the ability of other ERAD E3 complexes to destroy misfolded proteins would be compromised in the ER, rendering the ER more sensitive to stress.

It is interesting to note that overexpression of the dominant-negative gp78 not only renders liver more sensitive to tunicamycin-induced ER stress but also increases transcription of the Srebp target genes for lipogenesis and cholesterol synthesis. It is likely that these effects are mediated by ER stress-activated UPR. It is known that all three ER stress sensors: IRE1, PERK, and ATF6 can regulate lipid storage in the liver (Pagliassotti, 2012). The degree to which the UPR contribute to hepatic steatosis may depend on the cellular event that elicits UPR. Interestingly, overexpression of BiP, an inhibitor of UPR, has been shown to protect against insulin and ER stress-induced hepatic steatosis (Werstuck et al., 2001). Importantly, overexpression of BiP in mice also inhibits the activation of SREBP-1c (Ron and Walter, 2007; Kammoun et al., 2009). It is also possible that gp78 may directly regulate Srebp expression through modifying unknown substrate proteins. This possibility is supported by the fact that overexpression of the wild-type gp78 in liver reduced the expression of Srebp target genes to the levels below the basal level of expression. However, a recent study showed that inhibition of gp78 function in liver by liver-specific deletion of *gp78* gene decreased Srebp target gene expression and reduced lipid levels (Liu et al., 2012). The mechanism underlying this discrepancy remains to be determined.

Adult zebrafish were raised and maintained at the zebrafish facility of the Aquaculture Research Center, Institute of Marine and Environmental Technology, USA, as previously described (Li et al., 2011). Briefly, the fish were maintained at 28°C with 14 h of light and 10 h of dark, in 8 gallon aquaria supplied with freshwater and aeration. Fish embryos were exposed to 1 μg/mL of tunicamycin dissolved in dimethyl sulfoxide (DMSO) for 48 h between 3−5 dpf. Two to three month-old fish were exposed to 1 μg/mL tunicamycin in 50 mL fresh fish water for the indicated time described in the results section at 28°C during the day.

Total RNA was extracted from 5 dpf zebrafish larvae using Trizol reagent (Invitrogen, CA, USA). A rapid amplification of cDNA ends (RACE) cDNA library was made from purified total RNA using a cDNA kit (Fermentas, MD, USA). Zebrafish *gp78* cDNA was cloned from the 5′ RACE library using a 5′ GP78-P1 primer and a 3′ GP78-P2 primer (Table S1) that has a C-terminal *myc* tag sequence followed by the stop codon. The PCR products were purified and cloned into the pGEM-T easy vector (Promega, USA) to generate the pGEM-gp78 plasmid.

DNA plasmids for making probes were generated by PCR amplification from a cDNA library generated from 5 dpf larvae. All primers are listed in the Table S1. The PCR products were cloned into pGEM-T easy vector and sequenced. Followed by linearization with appropriate restriction enzymes (Table S2), the antisense RNAs were transcribed with either SP6 or T7 RNA polymerase using a digoxigenin RNA labeling mix (Roche, USA). The antisense probe for fatty acid binding

protein 10a (*fabp10a*) was generated as described previously (Bian et al., 2011). Whole-mount *in situ* hybridization was performed as described (Du and Dienhart, 2001).

The *gp78* translation blocker morpholino (gp78-5′-UTR-MO) was targeted to the 5′-untranslated region (UTR). The gp78-5′-UTR-MO (CAGTCCACACGTACAGCAGTCTTCT) was purchased from Gene Tools (Philomath, OR, USA) and used as described previously (Nasevicius and Ekker, 2000).

Morpholino antisense oligos were dissolved in Danieau buffer (Nasevicius and Ekker, 2000) to a final concentration of 0.5 mmol/L. Zebrafish embryos were injected at the 1- or 2-cell stage with 1−2 nL (5−10 ng) of MO as described previously (Xu et al., 2012). 1−2 nL of DNA (100 ng/μL) was co-injected with Tol2 transposase mRNA (50 ng/μL) into zebrafish embryos at the 1- or 2-cell stage.

To generate a DNA construct expressing a myc-tagged gp78, the *gp78* coding sequence with the myc tag sequence was re-amplified using BamHI-gp78-p1 and NotI-gp78-myc-p2 primers (Table S1). The amplified PCR product was directly cloned into pBSSK(+) through blunt end ligation using the *Eco*R V site in the vector. The insert was then released from the pBSSK-*gp78* plasmid by *Not* I and *Bam*H I digestion. The DNA insert of *gp78* was then subcloned into the *Not* I and *Bam*H I sites of the T2AL200R150G vector (Urasaki et al., 2006), which contains an elongation factor 1 alpha (*ef1α*) promoter for ubiquitous expression, to produce the plasmid *Tol2-ef1α:gp78-wt*^{myc}. The *Tol2-ef1α:gp78-R2M*^{myc} construct (Fig. S3A) expressing a gp78 dominant-negative mutant was generated by substitution of the H354 and H357 residues in the RING finger domain with asparagine residues using the QuickChange Site-directed Mutagenesis Kit (Stratagene, CA, USA). All constructs were confirmed by sequencing.

To generate DNA constructs expressing a myc-tagged gp78 under a liver specific promoter (Fig. S1A), the *ef1α* promoter in *Tol2-eflα:gp78-wt*^{myc} and *Tol2-eflα:gp78-R2M*^{myc} constructs were replaced with a liver specific promoter derived from the 5′ flanking sequence of the *Hef2*/*RGM* gene encoding the Hemochromatosis type 2 protein (Bian et al., 2011). Hef2 is also called Repulsive-Guidance Molecule C (RGM), and consequently, the plasmids were named *Tol2-RGM:gp78-wt*^{myc} and *Tol2-RGM:gp78-R2M*^{myc}. In brief, a 6-kb *RGM* promoter was amplified with primers RGM-p-XhoI-p1 and RGM-p-XhoI-p2 (Table S1) and then subcloned to pGEM-T easy vector to generate pGEM-RGMp construct. *Xho* I-digested RGM-promoter was released from pGEM-RGMp and subcloned into *Xho* I digested *Tol2-eflα:gp78-wt*^{myc} to produce a plasmid *Tol2-RGM:gp78-wt*^{myc}. *Tol2-RGM:gp78-R2M*^{myc} construct was generated by site-directed mutagenesis using primers gp78-Mu-P1 and gp78-Mu-P2 (Table S1). Production of *Tg(RGM:gp78-wt*^{myc}*)* and *Tg(RGM:gp78-R2M*^{myc}*)* transgenic fish was performed as described in the production *of Tg (ef1α:gp78*^{myc}*)* and *Tg(ef1α:gp78-R2M*^{myc}*)* transgenic fish.

Total RNA was isolated from zebrafish embryos at 0, 3, 6, 12, 14, 19, and 24 hpf and 2, 3, 4, 5, and 6 dpf with the Trizol reagent (Invitrogen). 1 μg of total RNA was used for the cDNA synthesis using the first-strand cDNA synthesis kit in a 20 μL reaction (Fermentas, USA). 1 μL of synthesized cDNA product was used for PCR analysis. For semi-quantitative RT-PCR, the synthesized cDNA was diluted 10-fold and 1 μL of diluted cDNA was used for PCR analysis. All 12.5 μL of PCR reaction solutions were used in DNA agarose gel electrophoresis. Primers and PCR cycles are listed in Table S1. The band intensities were quantified with free NIH Image J software.

Immunostaining was carried out using whole-mount zebrafish embryos as described previously (Tan et al., 2006) with an anti-myc antibody (9E10, Developmental Hybridoma Bank, USA). The secondary antibody was a biotinylated anti-mouse IgG (Vector Laboratories, CA, USA). Signal was detected using the avidin-biotin-peroxidase/diaminobezidine (ABC-DAB) assay (ABC, Vector Laboratories, Burlingame, CA, USA). The embryos were photographed under an upright microscope (Leica MZ12, Wetzlar, Germany) equipped with an Olympus DP70 Digital Microscope Camera (Olympus America Inc., NY, USA).

To produce a flag-tagged zebrafish gp78, the *gp78* coding sequence was re-amplified using HindIII-gp78-p1 and BamHI-gp78-p2 primers (Table S1). The amplified PCR product was subcloned to pFLAG-CMV6a vector through *Hind* III *and Bam*H I cutting sites. Flag-tagged human gp78 and myc-tag mouse MmUBC7 constructs were described previously (Fang et al., 2001; Tiwari and Weissman, 2001). HeLa cells grown on slide glass were transiently co-transfected with plasmids encoding flag-h-gp78 or flag-zf-gp78 with myc-MmUBC7. Twenty-four hours after transfection, cells were fixed in 4% paraformaldehyde for 30 min at 4°C and blocked in 0.1% saponin, 0.1% human serum albumin. The cells were labeled with mouse monoclonal anti-FLAG antibody and rabbit monoclonal anti-myc antibody for 1 h following labeled

with Alexa® Fluor 488 conjugated goat anti-mouse IgG (H + L) and Alexa® Fluor 594 conjugated with goat anti rabbit IgG (H + L) for 1 h. Fluorescence microscopy was performed using a Zeiss 510 Laser Scanning Confocal Microscope.

Wild-type or MO-injected zebrafish embryos at 24 hpf (100 embryos each) and 48 hpf (50 embryos each) were dechorionated manually and crushed gently to remove the yolk by triturating with a glass pipette. Embryos at 96 hpf (30 embryos each) and 120 hpf (20 embryos each) were directly used for protein extraction. All embryos were solubilized in 200 μL sodium dodecyl sulfate (SDS) loading buffer (0.125 mol/L Tris-HCl, pH 6.8, 4% SDS, 20% glycerol, 0.2 mol/L dithiothreitol (DTT), 0.02% bromophenol blue) containing 1 mmol/L phenylmethanesulfonyl fluoride (PMSF) as a protease inhibitor. Samples (20 μL each) were vortexed, and the proteins were separated on a 10% SDS-polyacrylamide gel electrophoresis (PAGE) gel. Adult fish liver, brain, heart, pancreas, ovaries, and muscle were dissected from 3-month-old wild-type female fish and snap-frozen in liquid nitrogen and stored at −80°C. Dissected organs were homogenized in buffer consisting of 20 mmol/L 4-(2-hydroxyethyl)-1-piperazineethanesulfonic acid) HEPES-KOH (pH 7.4), 100 mmol/L KCl, 2 mmol/L EDTA, 1 mmol/L PMSF, 1 mmol/L dithiothreitol, 10 μg/mL leupeptin, 1 μg/mL pepstatin A, and 1% Triton X-100. The liver protein samples (20−40 μg) were used in each lane. Adult fish livers were dissected from female wild-type or transgenic fish at 2 to 3 months of age and snap-frozen in liquid nitrogen and stored at −80°C. Protein extraction was carried out as described above. Proteins were electrophoretically transferred onto a Polyvinylidene fluoride (PVDF) membrane (Immobilon-P; Millipore, MA, USA). Immunodetections were carried out using the anti-gp78 monoclonal antibody 1F1 (Yang et al., 2010), anti-BiP (1:3000; Sigma, USA), and anti-γ-tubulin (1:2000; Sigma) antibodies and followed by incubation with peroxidase-conjugated secondary antibodies. The band intensities were quantified with NIH Image J software.

In vitro ubiquitination assay was described previously (Yang et al., 2010). To generate a pGEX-4T-gp78C construct that encodes GST-tagged cytosolic part of zebrafish gp78, primers BamHI-gp78C-P1 and XhoI-gp78C-P2 were designed (Table S1). Expression and purification of 6× histidine (his)-tagged gp78C and GST-tagged-zf-gp78C were performed as previously described (Fang et al., 2001).

In vitro ubiquitination was performed as described (Fang et al., 2001). In brief, E1 (60 nmol/L), Ube2g2 (200 nmol/L), ubiquitin (10 μmol/L) were incubated with gp78C (2 μg) in a 20 μL reaction system at 37°C in buffers containing 25 mmol/L Tris-HCl (pH 7.4), 2 mmol/L ATP, and 2 mmol/L $MgCl_2$, and 2 μL of the reaction mix were sampled at indicated time and subjected to treatment with the same volume of 2 × SDS sample buffer at 95°C for 5 min. Ubiquitin (Ub) chains were detected by immunostaining with anti-Ub monoclonal antibody (P4D1, sc-8017, Santa Cruz Biotechnology, USA).

This work was supported by the National Science Foundation (No. 1120833) to SF and a research grant (MB-8716-08) from United States−Israel Binational Agriculture Research and Development Fund to SD.

Table S1. List of primers, their sequences and PCR cycles.
Table S2. Generation of antisense probes.
Fig. S1. Liver specific overexpression of *gp78-R2M* in transgenic fish.
Fig. S2. Liver specific overexpression of gp78-wt in transgenic fish.
Fig. S3. Overexpression of gp78-wt and gp78-R2M in transgenic lines.
Supplementary data related to this article can be found at http://dx.doi.org/10.1016/j.jgg.2014.05.005.

Amano, T., Yamasaki, S., Yagishita, N., Tsuchimochi, K., Shin, H., Kawahara, K., Aratani, S., Fujita, H., Zhang, L., Ikeda, R., Fujii, R., Miura, N., Komiya, S., Nishioka, K., Maruyama, I., Fukamizu, A., Nakajima, T., 2003. Synoviolin/Hrd1, an E3 ubiquitin ligase, as a novel pathogenic factor for arthropathy. Genes Dev. 17, 2436−2449.

Ballar, P., Ors, A.U., Yang, H., Fang, S., 2010. Differential regulation of CFTRDeltaF508 degradation by ubiquitin ligases gp78 and Hrd1. Int. J. Biochem. Cell Biol. 42, 167−173.

Ballar, P., Shen, Y., Yang, H., Fang, S., 2006. The role of a novel p97/valosin-containing protein-interacting motif of gp78 in endoplasmic reticulum-associated degradation. J. Biol. Chem. 281, 35359−35368.

Bernardi, K.M., Williams, J.M., Kikkert, M., van Voorden, S., Wiertz, E.J., Ye, Y., Tsai, B., 2010. The E3 ubiquitin ligases Hrd1 and gp78 bind to and promote cholera toxin retro-translocation. Mol. Biol. Cell 21, 140−151.

Bian, Y.H., Xu, C., Li, J., Xu, J., Zhang, H., Du, S.J., 2011. Development of a transgenic zebrafish model expressing GFP in the notochord, somite and liver directed by the *hfe2* gene promoter. Transgenic Res. 20, 787−798.

Chen, Z., Du, S., Fang, S., 2012. gp78: a multifaceted ubiquitin ligase that integrates a unique protein degradation pathway from the endoplasmic reticulum. Curr. Protein Pept. Sci. 13, 414−424.

Cinaroglu, A., Gao, C., Imrie, D., Sadler, K.C., 2011. Activating transcription factor 6 plays protective and pathological roles in steatosis due to endoplasmic reticulum stress in zebrafish. Hepatology 54, 495−508.

Das, R., Mariano, J., Tsai, Y.C., Kalathur, R.C., Kostova, Z., Li, J., Tarasov, S.G., McFeeters, R.L., Altieri, A.S., Ji, X., Byrd, R.A., Weissman, A.M., 2009. Allosteric activation of E2-RING finger-mediated ubiquitylation by a structurally defined specific E2-binding region of gp78. Mol. Cell 34, 674−685.

Du, S.J., Dienhart, M., 2001. Gli2 mediation of hedgehog signals in slow muscle induction in zebrafish. Differentiation 67, 84−91.

Fang, S., Ferrone, M., Yang, C., Jensen, J.P., Tiwari, S., Weissman, A.M., 2001. The tumor autocrine motility factor receptor, gp78, is a ubiquitin

protein ligase implicated in degradation from the endoplasmic reticulum. Proc. Natl. Acad. Sci. USA 98, 14422−14427.

Fisher, E.A., Khanna, N.A., McLeod, R.S., 2011. Ubiquitination regulates the assembly of VLDL in HepG2 cells and is the committing step of the apoB-100 ERAD pathway. J. Lipid Res. 52, 1170−1180.

Fu, M., Li, L., Albrecht, T., Johnson, J.D., Kojic, L.D., Nabi, I.R., 2011. Autocrine motility factor/phosphoglucose isomerase regulates ER stress and cell death through control of ER calcium release. Cell Death Differ. 18, 1057−1070.

Howarth, D.L., Vacaru, A.M., Tsedensodnom, O., Mormone, E., Nieto, N., Costantini, L.M., Snapp, E.L., Sadler, K.C., 2012. Alcohol disrupts endoplasmic reticulum function and protein secretion in hepatocytes. Alcohol Clin. Exp. Res. 36, 14−23.

Joshi, B., Li, L., Nabi, I.R., 2010. A role for KAI1 in promotion of cell proliferation and mammary gland hyperplasia by the gp78 ubiquitin ligase. J. Biol. Chem. 285, 8830−8839.

Kammoun, H.L., Chabanon, H., Hainault, I., Luquet, S., Magnan, C., Koike, T., Ferre, P., Foufelle, F., 2009. GRP78 expression inhibits insulin and ER stress-induced SREBP-1c activation and reduces hepatic steatosis in mice. J. Clin. Invest. 119, 1201−1215.

Kim, S.M., Acharya, P., Engel, J.C., Correia, M.A., 2010. Liver cytochrome P450 3A ubiquitination *in vivo* by gp78/autocrine motility factor receptor and C terminus of Hsp70-interacting protein (CHIP) E3 ubiquitin ligases: physiological and pharmacological relevance. J. Biol. Chem. 285, 35866−35877.

Kostova, Z., Tsai, Y.C., Weissman, A.M., 2007. Ubiquitin ligases, critical mediators of endoplasmic reticulum-associated degradation. Semin. Cell Dev. Biol. 18, 770−779.

Li, H., Xu, J., Bian, Y.H., Rotllant, P., Shen, T., Chu, W., Zhang, J., Schneider, M., Du, S.J., 2011. Smyd1b_tv1, a key regulator of sarcomere assembly, is localized on the M-line of skeletal muscle fibers. PLoS ONE 6, e28524.

Li, W., Tu, D., Li, L., Wollert, T., Ghirlando, R., Brunger, A.T., Ye, Y., 2009. Mechanistic insights into active site-associated polyubiquitination by the ubiquitin-conjugating enzyme Ube2g2. Proc. Natl. Acad. Sci. USA 106, 3722−3727.

Lieschke, G.J., Currie, P.D., 2007. Animal models of human disease: zebrafish swim into view. Nat. Rev. Genet. 8, 353−367.

Liu, T.F., Tang, J.J., Li, P.S., Shen, Y., Li, J.G., Miao, H.H., Li, B.L., Song, B.L., 2012. Ablation of gp78 in liver improves hyperlipidemia and insulin resistance by inhibiting SREBP to decrease lipid biosynthesis. Cell Metab. 16, 213−225.

Malhotra, J.D., Kaufman, R.J., 2007. The endoplasmic reticulum and the unfolded protein response. Semin. Cell Dev. Biol. 18, 716−731.

Mehnert, M., Sommer, T., Jarosch, E., 2010. ERAD ubiquitin ligases: multifunctional tools for protein quality control and waste disposal in the endoplasmic reticulum. Bioessays 32, 905−913.

Morito, D., Hirao, K., Oda, Y., Hosokawa, N., Tokunaga, F., Cyr, D.M., Tanaka, K., Iwai, K., Nagata, K., 2008. Gp78 cooperates with RMA1 in endoplasmic reticulum-associated degradation of CFTRDeltaF508. Mol. Biol. Cell 19, 1328−1336.

Nasevicius, A., Ekker, S.C., 2000. Effective targeted gene 'knockdown' in zebrafish. Nat. Genet. 26, 216−220.

Pagliassotti, M.J., 2012. Endoplasmic reticulum stress in nonalcoholic Fatty liver disease. Annu. Rev. Nutr. 32, 17−33.

Passeri, M.J., Cinaroglu, A., Gao, C., Sadler, K.C., 2009. Hepatic steatosis in response to acute alcohol exposure in zebrafish requires sterol regulatory element binding protein activation. Hepatology 49, 443−452.

Peer, C.J., Sissung, T.M., Figg, W.D., 2011. CHIP and gp78-mediated ubiquitination of CYP3A4: implications for the pharmacology of anticancer agents. Cancer Biol. Ther. 11, 549−551.

Ponting, C.P., 2000. Proteins of the endoplasmic-reticulum-associated degradation pathway: domain detection and function prediction. Biochem. J. 351 (Pt 2), 527−535.

Ron, D., Walter, P., 2007. Signal integration in the endoplasmic reticulum unfolded protein response. Nat. Rev. Mol. Cell Biol. 8, 519−529.

Sasagawa, Y., Yamanaka, K., Ogura, T., 2007. ER E3 ubiquitin ligase HRD-1 and its specific partner chaperone BiP play important roles in ERAD and developmental growth in *Caenorhabditis elegans*. Genes Cells 12, 1063−1073.

Shen, Y., Ballar, P., Apostolou, A., Doong, H., Fang, S., 2007. ER stress differentially regulates the stabilities of ERAD ubiquitin ligases and their substrates. Biochem. Biophys. Res. Commun. 352, 919−924.

Shen, Y., Ballar, P., Fang, S., 2006. Ubiquitin ligase gp78 increases solubility and facilitates degradation of the Z variant of alpha-1-antitrypsin. Biochem. Biophys. Res. Commun. 349, 1285−1293.

Shimizu, K., Tani, M., Watanabe, H., Nagamachi, Y., Niinaka, Y., Shiroishi, T., Ohwada, S., Raz, A., Yokota, J., 1999. The autocrine motility factor receptor gene encodes a novel type of seven transmembrane protein. FEBS Lett. 456, 295−300.

Song, B.L., Sever, N., DeBose-Boyd, R.A., 2005. Gp78, a membrane-anchored ubiquitin ligase, associates with Insig-1 and couples sterol-regulated ubiquitination to degradation of HMG CoA reductase. Mol. Cell 19, 829−840.

Tan, X., Rotllant, J., Li, H., De Deyne, P., Du, S.J., 2006. SmyD1, a histone methyltransferase, is required for myofibril organization and muscle contraction in zebrafish embryos. Proc. Natl. Acad. Sci. USA 103, 2713−2718.

Thakur, P.C., Stuckenholz, C., Rivera, M.R., Davison, J.M., Yao, J.K., Amsterdam, A., Sadler, K.C., Bahary, N., 2011. Lack of *de novo* phosphatidylinositol synthesis leads to endoplasmic reticulum stress and hepatic steatosis in cdipt-deficient zebrafish. Hepatology 54, 452−462.

Tiwari, S., Weissman, A.M., 2001. Endoplasmic reticulum (ER)-associated degradation of T cell receptor subunits. Involvement of ER-associated ubiquitin-conjugating enzymes (E2s). J. Biol. Chem. 276, 16193−16200.

Tsai, Y.C., Leichner, G.S., Pearce, M.M., Wilson, G.L., Wojcikiewicz, R.J., Roitelman, J., Weissman, A.M., 2012. Differential regulation of HMG-CoA reductase and Insig-1 by enzymes of the ubiquitin-proteasome system. Mol. Biol. Cell 23, 4484−4494.

Urasaki, A., Morvan, G., Kawakami, K., 2006. Functional dissection of the Tol2 transposable element identified the minimal *cis*-sequence and a highly repetitive sequence in the subterminal region essential for transposition. Genetics 174, 639−649.

Vembar, S.S., Brodsky, J.L., 2008. One step at a time: endoplasmic reticulum-associated degradation. Nat. Rev. Mol. Cell Biol. 9, 944−957.

Walter, P., Ron, D., 2011. The unfolded protein response: from stress pathway to homeostatic regulation. Science 334, 1081−1086.

Wang, Y., Guan, S., Acharya, P., Koop, D.R., Liu, Y., Liao, M., Burlingame, A.L., Correia, M.A., 2011. Ubiquitin-dependent proteasomal degradation of human liver cytochrome P450 2E1: identification of sites targeted for phosphorylation and ubiquitination. J. Biol. Chem. 286, 9443−9456.

Wei, C., Liu, J., Yu, Z., Zhang, B., Gao, G., Jiao, R., 2013. TALEN or Cas9-rapid, efficient and specific choices for genome modifications. J. Genet. Genomics 40, 281−289.

Werstuck, G.H., Lentz, S.R., Dayal, S., Hossain, G.S., Sood, S.K., Shi, Y.Y., Zhou, J., Maeda, N., Krisans, S.K., Malinow, M.R., Austin, R.C., 2001. Homocysteine-induced endoplasmic reticulum stress causes dysregulation of the cholesterol and triglyceride biosynthetic pathways. J. Clin. Invest. 107, 1263−1273.

Xu, J., Gao, J., Li, J., Xue, L., Clark, K.J., Ekker, S.C., Du, S.J., 2012. Functional analysis of slow myosin heavy chain 1 and myomesin-3 in sarcomere organization in zebrafish embryonic slow muscles. J. Genet. Genomics 39, 69−80.

Yagishita, N., Ohneda, K., Amano, T., Yamasaki, S., Sugiura, A., Tsuchimochi, K., Shin, H., Kawahara, K., Ohneda, O., Ohta, T., Tanaka, S., Yamamoto, M., Maruyama, I., Nishioka, K., Fukamizu, A., Nakajima, T., 2005. Essential role of synoviolin in embryogenesis. J. Biol. Chem. 280, 7909−7916.

Yang, H., Liu, C., Zhong, Y., Luo, S., Monteiro, M.J., Fang, S., 2010. Huntingtin interacts with the cue domain of gp78 and inhibits gp78 binding to ubiquitin and p97/VCP. PLoS ONE 5, e8905.

Ying, Z., Wang, H., Fan, H., Zhu, X., Zhou, J., Fei, E., Wang, G., 2009. Gp78, an ER associated E3, promotes SOD1 and ataxin-3 degradation. Hum. Mol. Genet. 18, 4268−4281.